

The bispectrum of the Lyman- α forest at $z \sim 2 - 2.4$ from a Large sample of UVES QSO Absorption Spectra (LUQAS) ^{*}

M. Viel ¹, S. Matarrese ^{2,3}, A. Heavens ⁴, M.G. Haehnelt ¹, T.-S. Kim ¹,
V. Springel ⁵ & L. Hernquist ⁶

¹ *Institute of Astronomy, Madingley Road, Cambridge CB3 0HA*

² *Dipartimento di Fisica ‘Galileo Galilei’, via Marzolo 8, I-35131 Padova, Italy*

³ *INFN, Sezione di Padova, via Marzolo 8, I-35131 Padova, Italy*

⁴ *Institute for Astronomy, University of Edinburgh, Blackford Hill, Edinburgh EH9 3HJ*

⁵ *Max-Planck-Institut für Astrophysik, Karl Schwarzschild-str. 1, Garching bei München, Germany*

⁶ *Harvard-Smithsonian Center for Astrophysics, 60 Garden Street, Cambridge, MA 02198, USA*

19 February 2019

ABSTRACT

We present a determination of the bispectrum of the flux in the Lyman- α forest of QSO absorption spectra obtained from LUQAS which consists of spectra observed with the high resolution Echelle spectrograph UVES. Typical errors on the observed bispectrum as obtained from a jack-knife estimator are $\sim 50\%$. For wavenumbers in the range $0.03 \text{ s/km} < k < 0.1 \text{ s/km}$ the observed bispectrum agrees within the errors with that of the synthetic absorption spectra obtained from numerical hydro-simulations of a Λ CDM model with and without feedback from star formation. Including galactic feedback changes the bispectrum by less than 10%. At smaller wavenumbers the associated metal absorption lines contribute about 50% to the bispectrum and the observed bispectrum exceeds that of the simulations. At wavenumbers $k < 0.03 \text{ s/km}$ second-order perturbation theory applied to the flux spectrum gives a reasonable (errors smaller than 30%) approximation to the bispectra of observed and simulated absorption spectra. The bispectrum of the observed absorption spectra also agrees, within the errors, with that of a randomized set of absorption spectra where a random shift in wavelength has been added to absorption lines identified with VPFIT. This suggests that for a sample of the size presented here, the errors on the bispectrum are too large to discriminate between models with very different 3D distribution of Lyman- α absorption. If it were possible to substantially reduce these errors for larger samples of absorption spectra, the bispectrum might become an important statistical tool for probing the growth of gravitational structure in the Universe at redshift $z \gtrsim 2$.

Key words: Cosmology: intergalactic medium – large-scale structure of universe – quasars: absorption lines

1 INTRODUCTION

The Lyman- α forest in the absorption spectra of high-redshift QSOs has been recognized as an important tool for studying the underlying matter distribution (see

Rauch 1998 and Weinberg et al. 1999 for excellent reviews). In a previous paper (Kim et al. 2003, K03) an analysis of the flux power-spectrum of a large sample of UVES QSO absorption spectra (LUQAS) has been presented. Here we investigate the bispectrum of the flux in a subset of these absorption spectra.

The bispectrum is the Fourier transform of the three-point correlation function. As the flux in the

^{*} Based on data taken from the ESO archive obtained with UVES at VLT, Paranal, Chile.

Lyman- α forest is a sensitive probe of the matter distribution it should probe the topology of the 3D matter distribution in more detail than the two-point correlation function or the power-spectrum. It also can be used as a complementary tool to determine cosmological parameters (e.g. Fry 1994; Verde et al. 2002) and maybe also the physical state of the IGM. Gravitational growth induces correlations between large scale modes and small scale power which can be probed by the bispectrum. Zaldarriaga et al. (2001) pointed out that these correlations may be used to discriminate between fluctuations due to large-scale structure in the matter distribution and those produced by non-gravitational processes such as fluctuations in the continuum emission of the quasar. Mandelbaum et al. (2003) showed that with the SDSS (Sloan Digital Sky Survey) QSO sample it should be possible to use higher order statistics such as the bispectrum to determine amplitude, slope and curvature of the slope of the matter power spectrum with an accuracy of a few percent provided systematic errors are under control.

The plan of the paper is as follows. In Section 2 we briefly describe our sample. In Section 3 we define the flux bispectrum and compare the data with hydro-dynamical simulations, an analytical prediction and randomized spectra. Section 4 contains a summary of our results.

2 THE DATA

The LUQAS sample consists of 27 spectra taken with the Ultra-Violet Echelle Spectrograph (UVES) on VLT (Paranal, Chile) over the period 1999–2002. The spectra were drawn from the ESO archive and are publicly available to the ESO community. The total redshift path of the sample is $\Delta z = 13.75$. The median redshift of the sample is $\langle z \rangle = 2.25$ and the number of spectra covering the median redshift is 17. The analysis of the bispectrum has been restrained to the redshift range $2 < z < 2.4$, where approximately 15 QSOs contribute. The reason for this is the strong dependence of the bispectrum on the mean flux. The typical S/N is ~ 50 .

The spectra were reduced with the ECHELLE/UVES environment of the software package MIDAS. Lists of HI absorption lines and associated metal absorption lines identified and fitted with VPFIT (Carswell et al.: <http://www.ast.cam.ac.uk/~rfc/vpfit.html>) were available for 8 and 13 QSOs, respectively. Five out of the eight QSOs with lists of HI absorption are in the redshift range for which we calculated the bispectrum of the flux. We have removed four damped/sub-damped Lyman- α systems before computing the bispectrum. For a more complete description of the sample and for the analysis of the flux power-spectrum and its evolution with redshift we refer to K03.

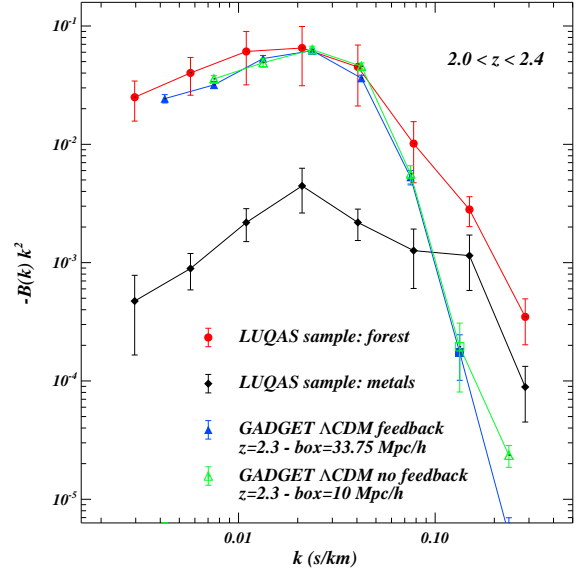


Figure 1. Filled circles show the one-dimensional bispectrum of the Lyman- α forest flux of the LUQAS sample in the redshift range $2 < z < 2.4$. The corresponding bispectrum of the associated metal absorption is shown by filled diamonds. Also shown is the flux bispectrum of synthetic spectra computed from hydro-dynamical simulations of a Λ CDM model at $z = 2.3$ (see Section 3.3). Filled triangles are for a simulation with a box size of $33.75 h^{-1}$ Mpc which include feedback from galactic winds. Empty triangles are for a simulation with box size of $10 h^{-1}$ Mpc without galactic feedback. Squares indicate positive values of $B(k)$. Errors are obtained with a jack-knife estimate.

3 THE BISPECTRUM OF THE Lyman- α FOREST

3.1 Method

We consider the quantity $\delta_F = (F - \langle F \rangle) / \langle F \rangle$, where F is the continuum fitted transmitted flux and $\langle F \rangle$ the average flux for each QSO (Hui et al. 2001, Croft et al. 2002). Note that δ_F corresponds to the flux estimator F_2 of K03. Dividing by the mean flux will adjust for differences in the mean flux level in a sample of spectra probing different redshifts.

We follow the definition of Matarrese, Verde & Heavens (1997) and Verde et al. (1998) for the bispectrum. We use the real part of the three point function in k -space, $D_F = \text{Re}(\delta_F(k_1) \delta_F(k_2) \delta_F(k_3))$, for closed triangles $k_1 + k_2 + k_3 = 0$. $\delta_F(k)$ is the Fourier transform of δF . D_F is related to the bispectrum of the flux $B_F(k_1, k_2, k_3)$

$$\langle D_F \rangle = 2\pi B_F(k_1, k_2, k_3) \delta^D(k_1 + k_2 + k_3). \quad (1)$$

$\delta^D(k)$ is the one-dimensional Dirac delta function and $\langle \cdot \rangle$ indicates the ensemble average. We compute the one-dimensional bispectrum. Our triangles are thus degenerate and we choose the configuration for which $k_1 = k_2$ and $k_3 = -2k_1$. In the following we will always show the flux bispectrum as a function of the wavenumber $k = k_1$.

3.2 The observed bispectrum

The filled circles in Fig. 1 show the one-dimensional bispectrum of the Lyman- α forest flux of the LUQAS sample in the redshift range $2 \leq z \leq 2.4$ plotted in dimensionless units (Table 1). The bin size was chosen such that visual comparison of different bispectra in the plots is not hindered by too large bin-to-bin fluctuations. As in K03 the error bars are computed with a jack-knife estimator, which gives results very similar to a bootstrap resampling of the data. Note that the bispectrum computed from the continuum fitted observed absorption spectra is negative. The same was found by Mandelbaum et al. (2003) for a statistic similar to the bispectrum in their analysis of synthetic spectra from numerical simulations. The negative sign of the bispectrum is expected if the higher order correlations arise from gravitational growth (Zaldarriaga et al. 2001).

For 13 of the 27 spectra we have metal line lists. From these lists we have produced artificial spectra which contain the metal lines only. The diamonds in Figure 1 show the mean bispectrum of these metal-line-only spectra which have a median redshift $z = 2.36$. For $k > 0.1$ s/km the identified metal lines contribute up to 50% to the bispectrum. At larger scales their contribution is considerably smaller.

We have also computed the flux bispectrum for the flux estimator F3 of K03 (see Figure 2 of K03), which is defined as $\delta_{F3} = \tilde{F}/\langle \tilde{F} \rangle - 1$, where \tilde{F} is the flux of the spectrum without continuum fitting. At $k < k_{\text{cont}} \sim 0.003$ s/km continuum fluctuations dominate the flux bispectrum and the values of the bispectrum become positive. The same was found by K03 for the flux power-spectrum. We therefore do not plot the bispectrum for $k < 0.003$ s/km.

3.3 Comparison with hydro-dynamical simulations

We have also calculated the bispectrum for synthetic spectra obtained from two outputs at $z = 2.3$ from the large set of hydro-dynamical simulations presented by Springel & Hernquist (2003a). The simulations were performed with the code GADGET (Springel, Yoshida & White 2001) modified to conserve entropy (Springel & Hernquist 2002) and are for a Λ CDM model with parameters $\Omega_0 = 0.3$ and $\Omega_\Lambda = 0.7$, Hubble constant $H_0 = 100 h \text{ km s}^{-1} \text{ Mpc}^{-1}$ with $h = 0.7$, baryon density $\Omega_b = 0.04$, a power spectrum with primordial spectral index $n = 1$, and rms fluctuation amplitude on $8h^{-1}$ Mpc scale, $\sigma_8 = 0.9$.

The simulation outputs are part of the O3 run and the D4 run. The O3 simulation has a box size of $10 h^{-1}$ Mpc box size, no feedback due to star formation and was performed with 2×144^3 particles. The D4 run has a box size of $33.75 h^{-1}$ Mpc, 2×216^3 particles and includes feedback by galactic winds. The mass of a gas particle is $3.72 \times 10^6 M_\odot$ and $4.24 \times 10^7 M_\odot$ in O3 and D4, respectively. Both simulations assume an UV background as modelled by Haardt & Madau (1996) and follow star formation with a hybrid multi-phase model (see Springel & Hernquist 2003b for details). Synthetic

spectra are extracted from the simulation in the usual way and are normalized to reproduce the effective optical depth $\tau_{\text{eff}} = -\ln\langle F \rangle = 0.165$ at $\langle z \rangle = 2.2$ in the observed spectra used for calculating the bispectrum.

The triangles in Fig. 1 show the flux bispectrum of the synthetic spectra with and without feedback from galactic winds. At $k < 0.1$ s/km the difference between the two simulations is smaller than 10%. This confirms that the feedback from high-redshift galaxies is expected to have little effect on the gas responsible for Lyman- α absorption (Theuns et al. 2002). This is most likely because the simulations mainly differ in the distribution of hot gas which has a small filling factor even for the simulation with feedback. The difference in box size and resolution also appear to have a little effect. For $k < 0.1$ s/km the bispectrum of synthetic and observed spectra agree within the errors. At larger wavenumbers the observed bispectrum exceeds that of the synthetic spectra. This is expected since at these wavenumbers the metal lines contribute significantly to the bispectrum (see Figure 1).

3.4 A second order perturbation theory approximation

In this section we will derive an analytical expression based on second-order perturbation theory which relates flux power spectrum and flux bispectrum and test it with synthetic spectra.

If the initial fluctuations are Gaussian and structures grow via gravitational instability the three-point correlation function is a second-order quantity. In the mildly non-linear regime second-order perturbation theory is a reasonable approximation (Matarrese *et al.* 1997). The structures which give rise to the Lyman- α forest have been shown to be mildly non-linear and to be reasonably well described by simple approximation schemes such as the log-normal model, at least on large scales (Bi & Davidsen 1997; Viel et al. 2002a, 2002b, 2003a; Matarrese & Mohayaee 2002).

In the Fluctuating Gunn-Peterson Approximation (FGPA; e.g. Hernquist et al. 1996) the flux can be related to the density field as

$$F = \exp[-A(1 + \delta_{IGM})^\beta], \quad (2)$$

where A and $\beta = 2 - 0.7(\gamma - 1)$ depend on z . γ is the power-law index of the gas temperature-density relation as usual. This assumes that redshift space distortions are not important (but see the extra effect of this assumption in Verde et al. 1998) and neglects thermal broadening and instrumental noise. Moreover, we assume that at the scales of interest $\delta_{IGM} \approx \delta_{DM} \approx \delta$. A more refined treatment, where these approximations are dropped, will be presented elsewhere.

Expanding the density field to second order as $\delta(\mathbf{x}) \approx \delta^{(1)}(\mathbf{x}) + \delta^{(2)}(\mathbf{x})$, and using the FGPA we get

$$\delta_F \approx b_1[\delta^{(1)}(\mathbf{x}) + \delta^{(2)}(\mathbf{x})] + \frac{b_2}{2}\delta^{(1)2}(\mathbf{x}), \quad (3)$$

with $b_1 = -A\beta$ and $b_2 = -A\beta(\beta - 1 - A\beta)$. The second-order quantity $\delta^{(2)}$ can be expressed as a quadratic

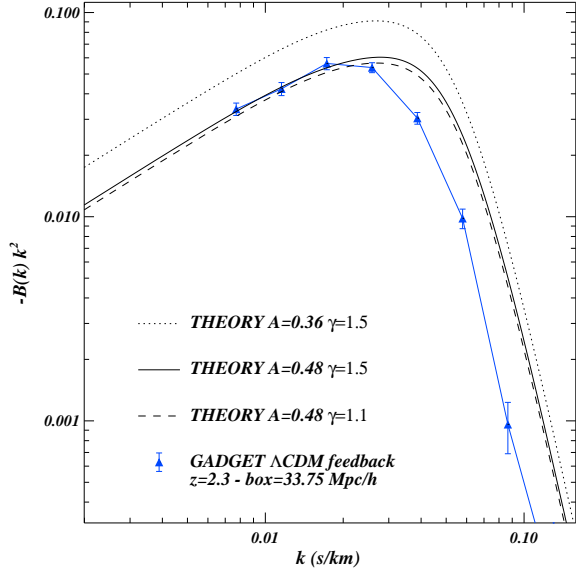


Figure 2. The flux bispectrum of the Lyman- α forest calculated from the flux power spectrum of synthetic spectra using the analytical relation of eq. (4). The continuous, dashed and dotted curves are for different parameter A and γ of the Fluctuating Gunn-Peterson Approximation (see text for details). Triangles show the bispectrum calculated directly from the synthetic spectra.

combination of linear perturbations $\delta^{(1)}$ with a suitable convolution kernel. The kernel is obtained by an expansion of the equations of gravitational instability up to second order (e.g. Catelan *et al.* 1995 and references therein). The expression for the Lyman- α bispectrum follows then by projecting the 3D bispectrum (e.g. Matarrese *et al.* 1997) along the line-of-sight,

$$\begin{aligned}
 B(k_1, k_2, k_3) &= \left(\frac{12}{7}c_1 + c_2\right) p(k_1)p(k_2) \\
 &+ c_1 \left[(k_1 k_2 - \frac{2}{7}k_1^2) p^{(-1)}(k_1) p(k_2)\right. \\
 &+ (k_2 k_1 - \frac{2}{7}k_2^2) p^{(-1)}(k_2) p(k_1) \\
 &\left. + \frac{6}{7}k_1^2 k_2^2 p^{(-1)}(k_1) p^{(-1)}(k_2)\right] + \text{cyc.}(1, 2, 3), \quad (4)
 \end{aligned}$$

where $c_1 = 1/b_1$, $c_2 = b_2/b_1^2$. $p(k)$ is the 1D flux power spectrum. The spectral moment $p^{(-1)}(k)$ is given by,

$$p^{(\ell)}(k) = |k|^{2\ell} p(k) + 2\ell \int_{|k|}^{\infty} dq q^{-2\ell-1} p(q) \quad (5)$$

with $\ell = -1$. Note that in the above eqs. k_1, k_2, k_3 have to be taken including their signs. The theoretical relation between the flux bispectrum and power-spectrum only depends upon the IGM parameters A and β . The very weak dependence on the matter density parameter Ω_m (e.g. Bouchet *et al.* 1992; Catelan *et al.* 1995) has been neglected as usual.

In Figure 2 we compare the bispectrum calculated from the 1D flux power spectrum of the synthetic spectra using eqs. (4) and (5) with the flux bispectrum calculated directly from the synthetic spectra. The rea-

son for choosing the simulated and not the observed spectra to test the accuracy of the analytical relation between bispectrum and power-spectrum is the significantly smaller errors of the bispectrum of the synthetic spectra. We have used synthetic spectra calculated from the D4 run of the numerical simulations (see Section 3.3). At $k < 0.03$ s/km the relation between bispectrum and power spectrum based on second-order perturbation theory is in good agreement with the simulations if we choose $A = 0.48$. The dashed and continuous curve are for $\gamma = 1.1$ and $\gamma = 1.5$, respectively. The differences between a value of $\gamma = 1.1$ and $\gamma = 1.5$ are very small. At $k > 0.03$ s/km the analytical prediction and the true bispectrum start to differ. This is probably due to neglect of the effects of thermal broadening and Jeans smoothing.

Note that that the value of A chosen for the analytical prediction of the bispectrum is different from the one in the synthetic spectra which was set to reproduce the observed mean flux decrement. The synthetic spectra were calculated with $A = 0.36$ and the analytical prediction of the bispectrum for this value is shown by the dotted curve in Figure 2. There is a clear discrepancy in the amplitude. We have tried to find the reason why the analytical prediction gives a good match for a somewhat different value of A without much success. We can only speculate that non-linear effects not properly taken into account by second-order perturbation theory are responsible.

3.5 The bispectrum for randomized absorption spectra

Viel *et al.* (2003b) have demonstrated that the Lyman- α forest flux power spectrum of “randomised” QSO absorption spectra is comparable in shape and amplitude to the flux power spectrum of the original observed spectra. They found that this is because of a large contribution of the shape of the Voigt profiles of discrete absorption systems to the flux power spectrum. We have performed here a similar test for the bispectrum. For 5 of the observed spectra in the redshift range where we have calculated the flux bispectrum we have a list of HI absorption lines obtained from Voigt profile fitting with VPFIT. For these we have produced 50 artificial randomized spectra each, where we have randomly shifted the hydrogen lines in wavelength. In Fig. 3 we compare the corresponding flux bispectrum to the flux bispectrum of the observed spectra. At $k < 0.1$ s/km they agree within the errors. A random superposition of Voigt profiles appears to reproduce the observed bispectrum similarly well as the numerical simulations. Metal lines were omitted in the reshuffled spectra hence the discrepancy at large wavenumbers. As in Viel *et al.* (2003) we have also calculated the bispectrum for randomized spectra where we halved and doubled the Doppler parameter of the lines. The result is similar. Broadening and narrowing of the lines leads to an approximately linear shift in wavenumber. This suggests that the bispectrum measures to a significant extent the shape of Voigt profiles. Note that the errors of the flux bispectrum are larger than that of the flux power spectrum. It is thus

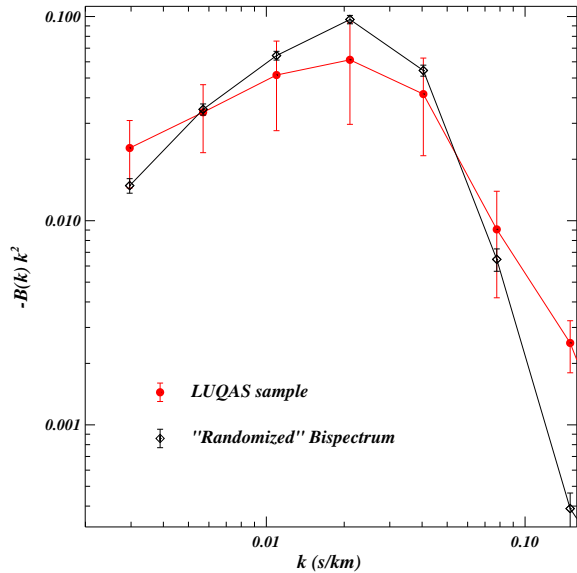


Figure 3. Comparison between the flux bispectrum of observed (filled circles) and “randomized” absorption spectra (empty triangles). The randomized absorption spectra have been obtained by randomly shifting the position of the absorption lines as obtained with VPFIT within the observed wavelength range. Error bars are jack-knife estimates.

more difficult to discriminate between the flux bispectrum of randomized spectra and the flux distribution of a CDM-like model than between the corresponding flux power spectra.

4 RESULTS AND DISCUSSION

We have computed the flux bispectrum of the LUQAS, sample a set of high resolution quasar spectra taken with UVES in the redshift range $2 < z < 2.4$, and compared to the flux bispectrum of synthetic spectra of a hydro-dynamical simulation and that of randomized spectra.

The main results are as follows:

- at wavenumbers $k < 0.1$ s/km the flux bispectrum of the observed spectra and that of synthetic spectra obtained of hydro-dynamical simulations of a Λ CDM model agree well within the errors (50%);
- including feedback from galactic winds has little effect on the flux bispectrum;
- at wavenumbers $k > 0.1$ s/km identified metal lines contribute significantly to the flux bispectrum (of the order 50 %), while at larger scales the contribution by metal lines is negligible;
- the analytical relation between the flux bispectrum and flux power spectrum based on second-order perturbation theory in the framework of the FGPA works well on scales $k < 0.03$ s/km for a normalization constant of the FGPA, $A \sim 0.5$ [eq. (2)], and a wide range of power-law indices of the temperature density relation, γ ;
- at wavenumbers $k < 0.1$ s/km the observed flux

Table 1. Flux bispectrum^(a) of the LUQAS sample in the redshift range $2.0 < z < 2.4$.

k (s/km)	$B(k)$ (km/s) ²
0.0030	-2845.669 ± 1057.042
0.0057	-1235.780 ± 434.839
0.0109	-507.897 ± 242.718
0.0210	-147.202 ± 76.589
0.0404	-27.551 ± 14.666
0.0777	-1.677 ± 0.894
0.1494	-0.126 ± 0.035
0.2872	-0.004 ± 0.001

(a) Bispectrum of the quantity $\delta_F = F / \langle F \rangle - 1$, where F is the observed continuum-fitted flux and $\langle F \rangle$ is the mean flux for each QSO, as computed from eq. (1).

bispectrum is consistent within the errors with that obtained for randomized spectra.

In summary, the observed bispectrum obtained from the LUQAS sample agrees similarly well with that of absorption spectra obtained from numerical simulations and randomized observed absorption spectra. This suggests that significantly larger samples of observed spectra as for example expected from SDSS and a tight control on systematic errors are necessary to utilize the bispectrum to constrain the 3D distribution of the absorbers and/or cosmological parameters. Analytical approximations based on second-order perturbation theory may be a promising tool in exploring the effect of gravitational growth on the flux bispectrum at large scales.

ACKNOWLEDGMENTS.

This work was supported by the European Community Research and Training Network “The Physics of the Intergalactic Medium”. We would like to thank ESO for making publicly available a superb set of QSO absorption spectra.

REFERENCES

- Bi H.G., Davidsen A.F., 1997, ApJ, 479, 523
 Bouchet F.R., Juszkiewicz R., Colombi S., Pellat R. 1992, ApJ, 394, L5
 Catelan P., Lucchin F., Matarrese S., Moscardini, L., 1995, MNRAS, 276, 39
 Croft R.A.C., Weinberg D. H., Bolte M., Burles S., Hernquist L., Katz N., Kirkman D., Tytler D., 2002, ApJ, 581, 20
 Fry J.N., 1994, Phys. Rev. Lett., Vol 73, N 2
 Haardt F., Madau P., 1996, ApJ, 461, 20
 Hernquist L., Katz N., Weinberg D.H., Miralda-Escude’ J., 1996, ApJ, 457, L51
 Hui L., Burles S., Seljak U., Rutledge R. E., Magnier E., Tytler D., 2001, ApJ, 552, 15
 Kim T.-S., Viel M., Haehnelt M.G., Carswell R.F., Cristiani S. 2003, astro-ph/0308103 (K03)
 Mandelbaum R., McDonald P., Seljak U., Cen R., 2003, astro-ph/0302112
 Matarrese S., Mohayaee R., 2002, MNRAS, 329, 37

- Matarrese S., Verde L., Heavens A., 1997, MNRAS, 290, 651
Rauch M., 1998, ARA&A, 36, 267
Springel V., Hernquist L., 2002, MNRAS, 333, 649
Springel V., Hernquist L., 2003a, MNRAS, 339, 312
Springel V., Hernquist L., 2003b, MNRAS, 339, 289
Springel V., Yoshida N., White S.D.M., 2001, New Astronomy, 6, 79
Theuns T., Viel M., Kay S., Schaye J., Carswell B., Tzanavaris P., 2002, ApJ, 578, L5
Verde L., Heavens A., Matarrese S., Moscardini L., 1998, MNRAS, 300, 747
Verde L. et al., 2002, MNRAS, 335, 432
Viel M., Matarrese S., Theuns T., Munshi D., Wang Y., 2003a, MNRAS, 340, L47
Viel M., Haehnelt M.G., Carswell R.F., Kim T.-S., 2003b, astro-ph/0308078
Viel M., Matarrese S., Mo H.J., Haehnelt M.G., Theuns T., 2002a, MNRAS, 329, 848
Viel M., Matarrese S., Mo H.J., Theuns T., Haehnelt M.G., 2002b, MNRAS, 336, 685
Weinberg D. et al., 1999, in: Evolution of large scale structure: from recombination to Garching, eds. A. J. Banday, R. K. Sheth, L. N. da Costa., p.346
Zaldarriaga M., Seljak U., Hui L., 2001, ApJ, 551, 48